Supplementary Material for

Effect of chemically induced fracturing on the ice nucleation activity of alkali feldspar.

Alexei Kiselev[1], Alice Keinert[1], Tilia Gaedeke[1], Thomas Leisner[1,2], Christoph Sutter[3], Elena Petrishcheva[3], Rainer Abart[3]

[1] Karlsruhe Institute of Technology, Institute of Meteorology and Climate Research, Karlsruhe, Germany
[2] Institut für Umweltphysik, Universität Heidelberg, Heidelberg, Germany
[3] University of Vienna, Department of Lithospheric Research, Althanstrasse 14, A-1090 Vienna, Austria

Correspondence to: Alexei Kiselev (alexei.kiselev@kit.edu)

Supplementary Figure 1. Microcline specimen used for preparation of FS06-010 sample. The cleavage planes were initially identified from the specimen appearance and angular relationships between the free growing planes and confirmed by back-scattered electron diffractometry (BSED).

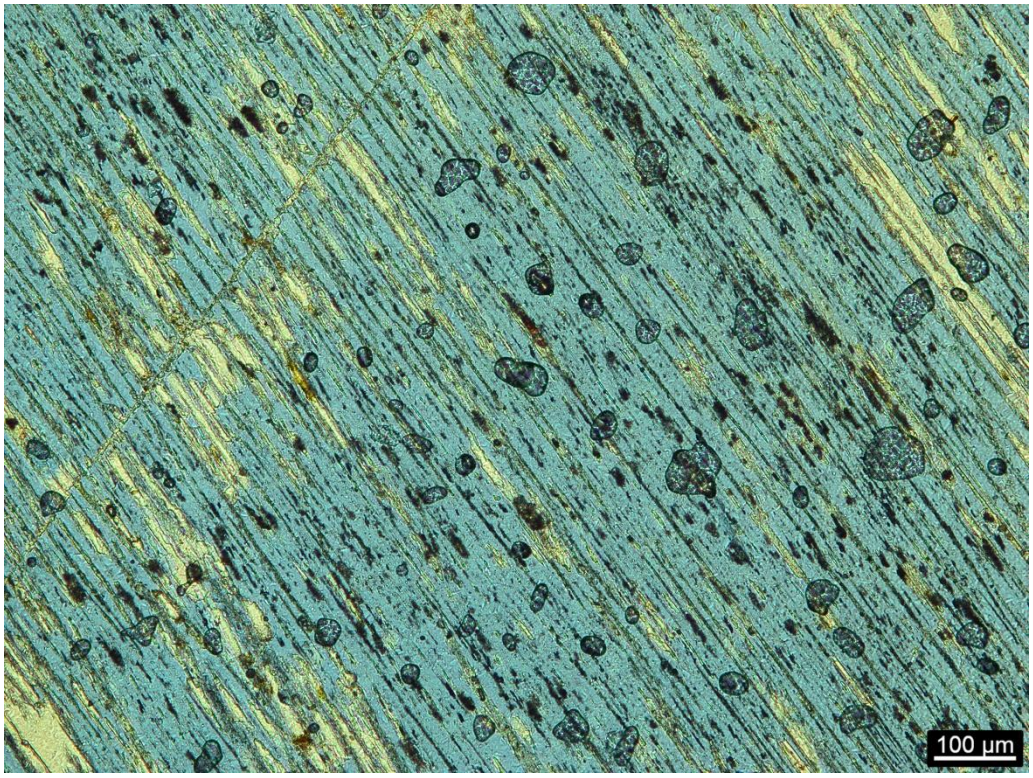

Supplementary Figure 2. Polarization microscope image of microcline feldspar (sample FS06-010). The thin section (~20 µm) was prepared parallel to the (010) plane. The micro-perthite structure of intergrowth lamellae is clearly visible. The interference colours are enhanced by the quartz wedge in the optical path of the microscope.

Supplementary Table 1. Lattice constants and fractional composition of FS06 sample determined with XRD (Panalytical, Cu K-alpha 1&2).

Components / Lattice constants	orthoclase	microcline	albite
a [Å]	**8.58499(28)**	8.59735(55)	8.14127(51)
b [Å]	**12.98310(27)**	12.97389(87)	12.7979(12)
c [Å]	**7.20553(16)**	7.21518(54)	7.15525(60)
α [°]	**90**	90.2851(84)	94.251(12)
β [°]	**116.0177(22)**	116.0222(65)	116.5891(74)
γ [°]	**90**	88.9051(72)	87.8129(94)
Volume [Å^3]	**721.736(35)**	723.066(95	664.82(10)
Fraction [%]	**41.08**	39.51	19.40

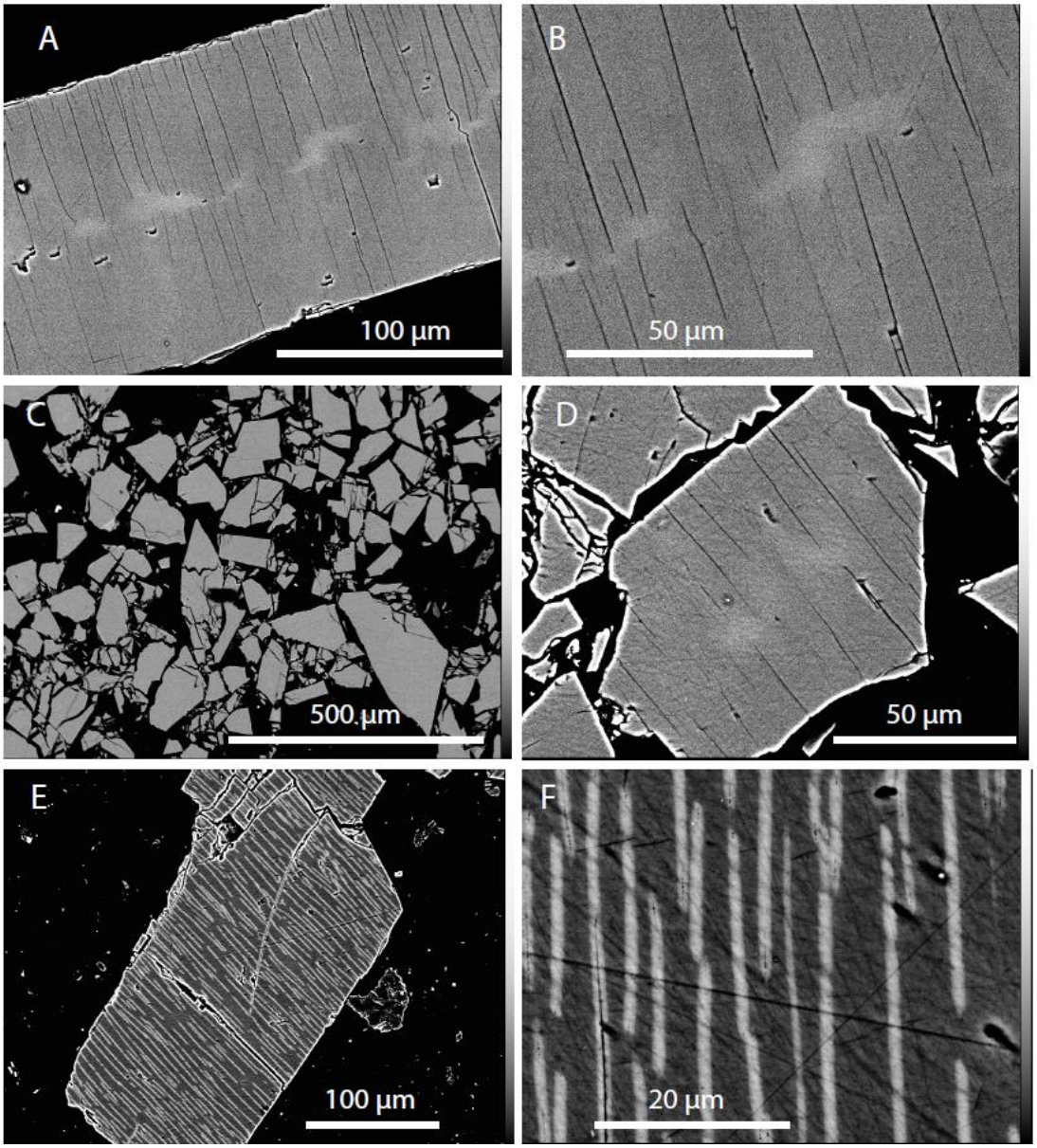

Supplementary Figure 3: Back-scattered electron (BSE) images of A: cation exchanged feldspar (sample F08-01), feldspar fragment bounded by (010) cleavage planes, with cracks extending approximately perpendicular to (010), cloud shaped light grey areas in the central portions are relic domains with relatively K-rich compositions; B: detail of the K-rich domain; C: overview image of grain mount of cation exchanged and subsequently vacuum annealed sample FS08-64c; D: detail of sample shown in C with well visible parallel cracks and relic cloud shaped K-rich domains in the central portion. E: overview of cation exchanged and subsequently salt annealed sample FS08-64o with well visible K-rich zones along previously formed cracks appearing bright grey in BSE contrast; F: detail of sample FS08-64o